MOLECULAR AND CELLULAR BIOLOGY, Aug. 1993, p. 4703–4713
0270-7306/93/084703-11$02.00/0

Vol. 13, No. 8

Evidence that the Middle T Antigen of Polyomavirus Interacts with the Membrane Skeleton

DAVID W. ANDREWS,* JYOTHI GUPTA, AND GIL ABISDRIS

Department of Biochemistry, McMaster University, 1200 Main Street West, Hamilton, Ontario L8N 3Z5, Canada

Received 17 November 1992/Returned for modification 5 February 1993/Accepted 19 May 1993

The transforming protein of polyomavirus, middle T antigen, is associated with cellular membranes. We have examined the subcellular location of the middle T antigen in two different cell types by fractionation and detergent phase partitioning. Middle T antigen expressed in human cells by a recombinant adenovirus was detected primarily in the membrane skeleton. Sucrose gradient fractionation revealed that the middle T antigen was associated with complexes with molecular weights of 500,000 to 1,000,000. Several markers for cytoskeleton cofractionate with these complexes, including actin, tubulin, and vimentin. Electron micrographs of membrane skeleton prepared from cells expressing middle T antigen demonstrated that this material contained primarily fibrous structures and was clearly devoid of bilayer membranes. These structures were distinct from the filamentous structures observed in fractions enriched for cytoskeleton. Consistent with a role for membrane skeleton localization in transformation, middle T antigen was detected exclusively in fractions enriched for membrane skeleton in middle T antigen-transformed Rat-2 cells. Our results may resolve the apparent difference between middle T antigen localization as determined by immunomicroscopy and that determined by subcellular fractionation.

The transforming protein of polyomavirus is the middle T antigen (mT). Analysis of a variety of cell lines and transgenic animals has demonstrated that mT is sufficient to transform both established cell lines and a wide variety of tissues (1, 39, 49, 51, 54). Mutational analyses suggest that the interaction of mT with cellular proteins is critical for transformation. In polyomavirus-infected cells, established cell lines expressing mT, and 293 cells infected with a recombinant adenovirus vector, mT has been shown to interact with members of the *src* family of tyrosine kinases (11, 15, 25, 29, 30, 35, 38), phosphoinositol-3-kinase (PI-3-kinase) (12, 19, 32, 36, 52), phosphatase 2A (22, 37, 50), and other as-yet-unidentified polypeptides. Complex formation with at least one member of the *src* family as well as with PI-3-kinase is necessary but not sufficient for transformation in vitro (11, 52). Association of mT with these molecules appears to activate both kinases (7, 45). Moreover, it appears that accumulation of the phosphorylated products of the PI-3-kinase is required for transformation (32). Nevertheless, only a fraction of mT molecules in cells are complexed to either the *src* family kinases or PI-3-kinase; therefore, it remains possible that additional interactions are involved in cellular transformation (23).

Subcellular fractionation, immunofluorescence, and immunoelectron microscopy of mT-expressing cells suggest that mT is found in association with subcellular membranes (4, 9, 18, 41, 44, 47, 55). It has been assumed that mT is an integral membrane protein because of a contiguous 22-amino-acid hydrophobic segment near the carboxyl end of the molecule. Mutations in this region of mT abrogate both membrane association and transformation (reviewed in reference 34). Because mT lacks a signal sequence at the amino terminus, it is unlikely that the molecule associates with membranes by the conventional secretory pathway. The hydrophobic carboxyl domain of mT resembles the transmembrane region of other molecules, and it is the only segment of the molecule that is both sufficiently hydrophobic and long enough to span a lipid bilayer. Therefore, it has been postulated that mT spontaneously associates with membranes in a manner analogous to cytochrome b_5 (40).

In contrast to most integral membrane proteins, membrane assembly of cytochrome b_5 proceeds posttranslationally and spontaneously via the insertion of a carboxyl-terminal hydrophobic domain into the lipid bilayer (5, 16). However, direct comparison of membrane association for the hydrophobic tails of cytochrome b_5 and mT revealed that the mT carboxyl domain does not mediate spontaneous membrane assembly in vitro (28a). Therefore, the mechanism of membrane interaction of mT is likely to be more complicated than is currently believed.

Introducing a charged residue into the mT hydrophobic sequence resulted in a transformation defect without abolishing membrane binding or stimulation of kinase activity (33). Furthermore, replacing the hydrophobic tail of mT with that of vesicular stomatitis virus glycoprotein G resulted in a chimeric molecule which sedimented with the particulate fraction of cells and exhibited associated kinase activity but was transformation negative (47). The results from these studies suggest that the mode of membrane attachment of mT may have direct consequences for transformation.

We have made use of a variety of cell fractionation procedures to examine the localization of mT in 293 cells after expression with an adenovirus vector and in a Rat-2 cell line transformed with a plasmid encoding mT. Our results suggest that the interaction of mT with membranes may involve components of the cytoskeleton. Furthermore, it appears that at least a fraction of mT forms a complex with proteins associated with the submembranous part of the cytoskeleton, referred to as the membrane skeleton. Identification of an interaction between mT and the membrane skeleton suggests that mT may participate directly in the alterations in cellular morphology that accompany transformation.

* Corresponding author.

MATERIALS AND METHODS

Biological reagents. The adenovirus vector encoding mT (Ad5mT/AE), a plasmid encoding mT (Psv2neoMT), and the Rat-2 cell line used in this work were kindly provided by J. Hassell, McMaster University. Monoclonal antibodies 701, 721, and 722 to mT were the generous gift of S. Dilworth, Royal Postgraduate Medical School, University of London, London, England (17). Human kidney cells (293 N3S) were provided by F. Graham, McMaster University. Monoclonal antibodies to adenovirus proteins were a gift from A. Wandeler, Animal Diseases Research Institute, Nepean, Ontario, Canada.

Polyclonal antibody to c-Src was from Cambridge Research Biochemicals; monoclonal antibodies to phosphotyrosine (PY20) and actin (C4) were from ICN ImmunoBiologicals. Anti-β-tubulin (KMX-1) and anti-vimentin (Vim 3B4 and V9) monoclonal antibodies were from Boehringer Mannheim. Secondary antibodies conjugated to alkaline phosphatase and horseradish peroxidase were from Jackson Immunoresearch Laboratories and Amersham, respectively.

Restriction endonucleases and DNA-modifying agents were purchased from New England Biolabs. Peroxide-free detergents were from Boehringer Mannheim. Radioisotopes ([^{35}S]methionine and [^{32}P]ATP) were from Dupont, NEN. Enzygraphic Web HS was purchased from International Biotechnologies Inc.

Polyclonal mT antiserum. A polyclonal antiserum was prepared in rabbits against a fragment of mT spanning amino acids 176 to 393. This fragment includes most of the modulatory domain of mT (34). An *Sph*I-*Bam*HI restriction fragment encoding this segment was subcloned into a modified version of the plasmid pGEX2-T (Pharmacia) to generate a fusion protein expressed in bacteria. The resulting plasmid, pSPGEXmT1, encodes 216 amino acids of mT fused to the carboxyl end of glutathione *S*-transferase. Expression of the fusion protein and purification were essentially as described previously (31), except that inclusion bodies were solubilized in 4 M urea. The resulting antisera were characterized for specific reaction with mT by immunoprecipitation of mT synthesized in reticulocyte lysate and on Western blots (immunoblots) of cell extracts by comparison with the previously characterized monoclonal antibodies 701, 721, and 722 (17) (data not shown [all data referred to as not shown were provided with the manuscript at the time of review]). Western blots probed with specific antisera were developed with secondary antibodies conjugated to alkaline phosphatase or horseradish peroxidase. Densitometry of these blots (by transmission with an LKB 2222-020 Ultroscan XL) was used to determine the linear range of alkaline phosphatase detection of mT. Wherever possible, the amount of material analyzed was chosen such that the major mT bands were near the middle of the linear region. Limitations in the amount of material that could be loaded on the sucrose gradients and the relative amount of cofractionating actin and mT made quantification from sucrose gradients difficult. For this reason, these blots have been interpreted qualitatively. Because the bands on blots fade over time, images of the blots were recorded with a video camera and Kontron image analysis system. Copies of the blots were reproduced with a thermal printer.

Cell culture and membrane preparation. Cells (293 N3S) were maintained in monolayer culture in F-11 minimal essential medium supplemented with 10% fetal calf serum, penicillin, streptomycin, and amphotericin B (Fungizone) (GIBCO). For expression of mT, 293 cells were infected with recombinant adenovirus Ad5mT/AE at a multiplicity of infection of 10 PFU per cell (13). Cells were harvested 18 h postinfection, washed in phosphate-buffered saline (PBS), and suspended in hypotonic buffer (10 mM HEPES [*N*-2-hydroxyethylpiperazine-*N*′-2-ethanesulfonic acid, pH 7.8], 15 mM KCl, 2 mM $MgCl_2$, 0.1 mM EDTA, 1 mM dithiothreitol, 1 mM phenylmethylsulfonyl fluoride, 0.1 μg of chymostatin per ml, 0.1 μg of antipain per ml, 0.1 μg of leupeptin per ml, 0.1 μg of pepstatin per ml, 1 U of aprotinin per ml) for 10 min on ice. In some samples, 0.1 mM sodium orthovanadate was included as a phosphatase inhibitor. The cells were disrupted with a Dounce homogenizer until 90 to 95% of the cells were broken (~30 strokes). Nuclei were removed by centrifugation at 1,000 × *g* for 5 min. After correcting for the number of unbroken cells, we estimated that approximately 25% of the total mT in the cell was discarded with the nuclear pellet. The supernatant was centrifuged at 100,000 × *g* for 1 h, and the resulting pellet (P100) was resuspended in 50 mM triethanolamine (pH 8.0)–1 mM dithiothreitol–0.25 M sucrose. Aliquots containing approximately 300 μg of protein (~100 μl) were stored at −70°C.

To generate lines of transformed cells, the plasmid PsvneoMT was transfected into normal Rat-2 cells by calcium phosphate precipitation (53). This plasmid contains the complete open reading frame for polyomavirus mT, the polyomavirus promoter, and the polyadenylation sequences. The plasmid also contains the neomycin resistance gene to permit selection of transfected cells. After selection with G418, individual colonies were picked and transferred to microtiter wells. Rat-2 cells were grown in Dulbecco's modified Eagle's medium supplemented as described above. Transfected cultures were maintained in G418 (400 μg/ml)-containing growth medium to establish cells harboring the exogenous mT gene. G418-resistant cells were assayed for focus formation, doubling time, growth in semisolid medium, and reduced serum requirements. Transformed colonies were expanded into cell lines, and P100 fractions were prepared from these cells as described above.

Extraction with sodium carbonate. P100 fractions were extracted essentially as described previously (21). Briefly, aliquots of approximately 100 μg of total protein were incubated in 5 ml of 0.1 M sodium carbonate (pH 11.5) for 30 min on ice. Samples were layered onto a 1.0 M sucrose cushion (250 μl) and were centrifuged at 350,000 × *g* for 30 min at 4°C. Ovalbumin (10 μg) was added as a carrier, and proteins in the supernatant were precipitated with trichloroacetic acid and solubilized in sodium dodecyl sulfate-polyacrylamide gel electrophoresis (SDS-PAGE) loading buffer. Pelleted material was either solubilized directly in SDS-PAGE loading buffer or prepared for electron microscopy as described below.

Detergent solubilization. P100 fractions containing 15 to 20 μg of protein were incubated in 400 μl of extraction buffer (10 mM Tris-HCl [pH 7.4], 150 mM NaCl, and the following protease inhibitors: 0.1 μg of chymostatin per ml, 0.1 μg of antipain per ml, 0.1 μg of leupeptin per ml, 0.1 μg of pepstatin per ml, 1 U of aprotinin per ml, and 1 mM phenylmethylsulfonyl fluoride) containing a 0.5 or 1.0% concentration of the specified detergent. Samples containing octylglucoside, Triton X-100, Nonidet P-40, CHAPS {3-[(3-cholamidopropyl)-dimethyl-ammonio]-1-propanesulfonate}, Nikkol, or RIPA buffer (10 mM Na_3PO_4 [pH 7.2], 150 mM NaCl, 1% Nonidet P-40, 0.1% sodium deoxycholate, 0.1% SDS, 2 mM EDTA) were incubated at ~0°C. Samples containing deoxycholate were incubated at 24°C to prevent

gelling of the detergent. Detergent-insoluble pellets were prepared by centrifugation at 150,000 × *g* for 15 min (28 lb/in^2 in a Beckman Airfuge A100/30 rotor). Proteins in the supernatant were precipitated with trichloroacetic acid and then washed extensively with an ice-cold solution containing 50% ethanol–50% ether (vol/vol). This washing step solubilizes most of the detergent that coprecipitates with the proteins. The insoluble proteins were repelleted by centrifugation for 15 min in a microcentrifuge, residual solvent was evaporated, and the pellets were prepared for SDS-PAGE. Samples were separated by SDS-PAGE with the Tris-Tricine buffer system (42), because protein migration in this buffer system was less affected by residual nonionic detergent. Electrophoresis conditions (time of separation and acrylamide concentration) were adjusted to give optimal separation in the range of 70 to 10 kDa.

Phase partitioning. Phase separation of proteins from P100 fractions was based on a method described previously (8). For infected 293 cells, 15 μg (5 μl) of protein was added to 200 μl of solubilization buffer (20 mM Tris-HCl [pH 7.4], 300 mM NaCl, 2% Triton X-114 [TX-114], 10% glycerol). After 5 min on ice, 195 μl of ice-cold sterile distilled water was added, and the mixture was incubated for an additional 15 min on ice. To prepare samples of small enough volume and containing sufficient mT for identification on blots of sucrose gradient fractions, it was necessary to solubilize 150 to 300 μg of protein (50 to 100 μl) in a final volume of 200 μl of solubilization buffer. Under these conditions, proteins were not separated as cleanly. For mT-transformed Rat-2 cells, 600 μg of protein in a P100 fraction was solubilized in 14 mM Tris-HCl (pH 7.4)–214 mM NaCl–1.4% TX-114–7% glycerol. After 5 min at 4°C, the reaction was adjusted to a final volume of 1 ml and contained 10 mM Tris-HCl (pH 7.4)–150 mM NaCl–1.0% TX-114–5% glycerol. This starting volume provided enough Rat-2-derived material for four or more electroblots. At each step in the procedure, protease inhibitors were added to both fractions such that the concentration of each was increased by 0.2 μg of chymostatin per ml, 0.2 μg of antipain per ml, 0.2 μg of leupeptin per ml, 0.2 μg of pepstatin per ml, 2 U of aprotinin per ml, and 1 mM phenylmethylsulfonyl fluoride. The protease inhibitors were added to replace those redistributed during phase partitioning.

After initial solubilization and incubation for 15 min on ice, the detergent-insoluble cytoskeleton was pelleted by centrifugation at 14,000 × *g* for 10 min. The supernatant was layered on a cushion containing an equal volume of 6% sucrose–10 mM Tris-HCl (pH 7.4)–150 mM NaCl–0.06% TX-114–1% glycerol and was incubated at 30°C for 3 min to separate the detergent from the aqueous phase. The detergent phase was then pelleted by centrifugation at 735 × *g* for 3 min. The aqueous phase was removed from the cushion, and TX-114 was added from a 10% stock such that the detergent concentration was increased by 0.5%. After gentle mixing, the solution was placed on ice for 3 min to ensure complete solubilization of the detergent. This material was then layered back on the same cushion used previously, the phases were separated by incubation at 30°C, and the detergent phase was collected by centrifugation as described above. The aqueous phase and one-half of the cushion were removed, and TX-114 was added as described above. After incubation on ice for 3 min to solubilize the detergent, this material was layered on a new sucrose cushion, the phases were separated, and the detergent phase was removed by centrifugation. This second detergent pellet was discarded. Membrane skeleton was isolated from the aqueous phase by centrifugation at 150,000 × *g* for 30 min at 4°C. Trichloroacetic acid was added to the supernatants to precipitate soluble proteins as described above.

The detergent phase (containing hydrophobic membrane proteins) was resuspended in wash buffer (10 mM Tris-HCl [pH 7.4], 150 mM NaCl) to a volume equal to the final aqueous phase. After incubation on ice for 3 min to solubilize the detergent, the mixture was layered on a sucrose cushion, phases were separated by incubation at 30°C for 3 min, and the detergent phase was collected by centrifugation as described above. The detergent pellet was resuspended once more in wash buffer, and proteins were precipitated with trichloroacetic acid. Typically, this phase separation strategy resulted in 70 to 80% recovery of the starting material. The distributions of P100 fraction proteins between the different fractions were roughly equivalent (20% of the total for each) for the cytoskeleton, membrane skeleton, and detergent phase. The remaining ~40% of P100 protein was recovered as soluble hydrophillic proteins in the post-membrane skeleton aqueous phase.

For separation of membrane skeleton complexes by sucrose density centrifugation, 200 μl of the TX-114 aqueous phase prepared from P100 membrane fraction was layered on 4.8-ml 10 to 60% sucrose gradients containing 10 mM Tris-HCl (pH 7.5), 150 mM NaCl, 0.1% TX-114, 1.0% glycerol, 1 mM dithiothreitol, and protease inhibitors as described above. Centrifugation was for 6 h at 115,000 × *g* (Beckman SW50.1 at 32,000 rpm). Gradients were divided into 10 to 12 fractions, as specified, by manually removing fractions from the top. Some variability was observed between experiments, in part reflected by changes in the positions of molecular weight (MW) markers (typically one fraction). Fractions were assayed for kinase activity before or after immunoprecipitation with antiserum specific to mT by adding [γ-^{32}P]ATP and 1 mM $MnCl_2$ and incubating at 30°C for 5 min. In control experiments, incubation of the TX-114 aqueous phase prior to sedimentation in sucrose gradients resulted in a small increase in the heterogeneity of the complexes detected on blots. However, the magnitude of the change due to incubation alone was much smaller than was detected with the active agents (compare the distributions for mT in Fig. 5A with those in Fig. 7A).

Electron microscopy. Cell fractions were prepared as described above and, where necessary, were pelleted by centrifugation at 150,000 × *g* for 30 min. Pellets were fixed with 2% glutaraldehyde in 0.1 M sodium cacodylate (pH 7.4) for 30 min at 4°C. The pellets were washed twice with cacodylate buffer and incubated with 1% osmium tetroxide for 1/2 h at 4°C. Samples were dehydrated and embedded in Spurr's resin. Thin sections (~90 nm) were stained with uranyl acetate and lead citrate. Pellets were sectioned obliquely to permit examination of the entire sample.

RESULTS

In a study of membrane assembly via carboxyl-terminal hydrophobic domains, we observed that the putative membrane anchor of mT is atypical in that it does not mediate the spontaneous association of polypeptides with membranes in vitro (28a). To examine membrane assembly of mT in whole cells, the protein was expressed in 293 cells by an adenovirus vector (13) and the protein was expressed in Rat-2 cells transformed by expression of mT by the plasmid Psv2neoMT. The adenovirus system provides a convenient source for relatively large amounts of membrane-associated protein (36). Moreover, a fraction of mT expressed in 293

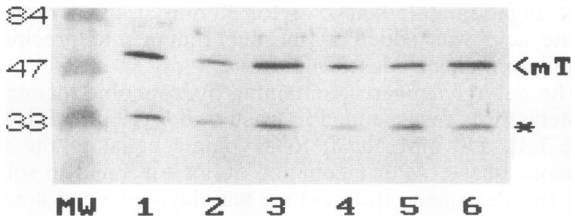

FIG. 1. Solubilization of mT in deoxycholate. Immunoblot probed with monoclonal antibodies 701, 721, and 722 (17) to mT. Approximately 15 μg of protein from a P100 fraction was added to 400 μl of solubilization buffer containing 0.5% (lanes 1 to 3) or 1.0% (lanes 4 to 6) deoxycholate. After solubilization, this material was separated by centrifugation into fractions enriched for cytoskeleton (lanes 1 and 4), soluble proteins (lanes 2 and 5), and membrane skeleton (lanes 3 and 6). Cytoskeleton was pelleted by centrifugation for 30 min at 14,000 × *g*. Membrane skeleton was pelleted from the post-cytoskeleton supernatant by centrifugation at 150,000 × *g* for 20 min. The migration position of mT is indicated at the right of the figure (<mT). The band of lower MW, indicated by the asterisk, is presumed to result from degradation of mT. Prestained MW markers indicate MWs of 84,000, 47,000, and 33,000.

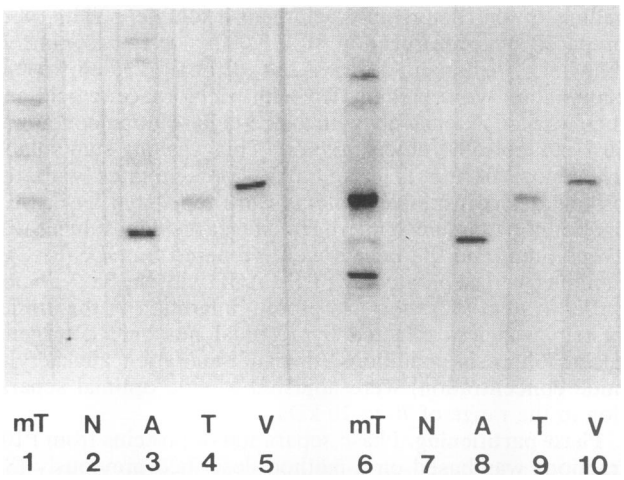

FIG. 2. Extraction of membranes with sodium carbonate (pH 11.5). Approximately 100 μg of total protein from a P100 fraction was incubated in 5 ml of 0.1 M sodium carbonate (pH 11.5) for 30 min on ice. Samples were layered onto a 1.0 M sucrose cushion (250 μl) and centrifuged at 350,000 × *g* for 30 min at 4°C. Proteins were collected from the supernatant by precipitation with trichloroacetic acid, washed with ethanol-ether (1:1), and prepared for SDS-PAGE (lanes 1 to 5). The pelleted material was solubilized in loading buffer, and proteins were separated by SDS-PAGE (lanes 6 to 10). After electrophoretic transfer to nitrocellulose, the resulting blot was probed with antibodies specific for mT (monoclonal antibodies 701, 721, and 722 [17]), actin (A), tubulin (T), and vimentin (V) with a Bio-Rad multiscreen. As a control, an irrelevant monoclonal antibody (N) was added (lanes 2 and 7). Antibody bands were detected with anti-rat and anti-mouse alkaline phosphatase-conjugated antibodies.

cells has been shown to complex with PI-3-kinase and *src* family kinases, suggesting that membrane assembly is similar to that seen in transformed cells (36).

To characterize the membrane-bound form of mT, vesicles were prepared from the cells as a P100 fraction. The mT in this fraction was analyzed by the standard biochemical criteria of extraction with nonionic detergent or high pH. A typical integral membrane protein is solubilized in 0.5 to 1.0% nonionic detergent but is resistant to extraction by pH 11.5 (8, 21). It has been shown that mT can be released from cells by solubilization in nonionic detergents (23, 41). However, as shown in Fig. 1, the mT released is not completely solubilized. In these experiments, the P100 membrane fraction was resuspended and added to solubilization buffer containing 0.5% (Fig. 1, lanes 1 to 3) or 1.0% (Fig. 1, lanes 4 to 6) deoxycholate. After solubilization, this material was separated into fractions enriched for cytoskeleton (Fig. 1, lanes 1 and 4), the submembranous filamentous network termed the membrane skeleton (Fig. 1, lanes 3 and 6), and soluble proteins (Fig. 1, lanes 2 and 5). The relative amount of mT present in each fraction was determined by immunoblotting.

To enrich for cytoskeleton, detergent-insoluble material was pelleted by centrifugation for 30 min at 13,000 rpm (approximately, 14,000 × *g*) in a microcentrifuge (20). At 0.5% deoxycholate, 47% of the mT in the P100 fraction is recovered in this fraction. However, at 1.0% deoxycholate, solubilization is more effective and only 26% of the mT in this fraction is recovered (Fig. 1, compare lanes 1 and 4). At 1.0% detergent, the majority of mT (48%) is recovered with the membrane skeleton (material pelleted from the post-cytoskeleton supernatant by centrifugation at 150,000 × *g* for 20 min) (Fig. 1, lane 6). Nevertheless, 14 and 25% of the mT remains in the soluble fraction at the two detergent concentrations, respectively (Fig. 1, lanes 2 and 5). The lower-MW mT immunoreactive band in each of the lanes is presumed to result from degradation of mT. Densitometry of the blot in Fig. 1 demonstrated that, on average, 30% of the mT immunoreactive material was present in the lower-MW form. However, if the distribution of mT between fractions is calculated with or without the putative degradation product, the relative distribution changes by less than 5%. Moreover, control experiments demonstrated that essentially all of the mT in an equal number of cells washed in ice-cold PBS and then lysed directly in SDS-PAGE loading buffer was accounted for in these fractions and the nuclear pellet. Therefore, the distribution of mT inferred from that of the full-length mT detected in these blots is likely to represent distribution of at least 70% of the mT expressed in infected 293 cells rather than a specific protease-resistant subfraction. Similar results were obtained with Triton X-100, Nonidet P-40, octylglucoside, Nikkol (data not shown), and TX-114 (see below). As expected, detergent combinations containing SDS (such as RIPA buffer) solubilized essentially all of the mT (data not shown).

Integral membrane proteins can be distinguished from peripheral membrane proteins and proteins located in the lumen of vesicles by resistance of the former to extraction at pH 11.5 (21). When assayed with 100 mM sodium carbonate (pH 11.5), the mT present in the P100 fraction was recovered primarily in the membrane pellet fraction (Fig. 2, compare lane 1 and lane 6). Electron micrographs of this fraction confirmed that exposure to high pH had removed peripheral structures (such as ribosomes) and converted membrane vesicles to smooth sheetlike structures (data not shown). On the basis of previous descriptions of carbonate-extracted membranes, we did not expect to detect cytoskeleton or membrane skeleton in this fraction (21). Structures similar to cytoskeleton were not observed in electron micrographs of membranes extracted with sodium carbonate (data not shown; also see reference 21). However, when the nitrocellulose blot was probed with antisera to proteins common to both cytoskeleton and membrane skeleton, actin, tubulin,

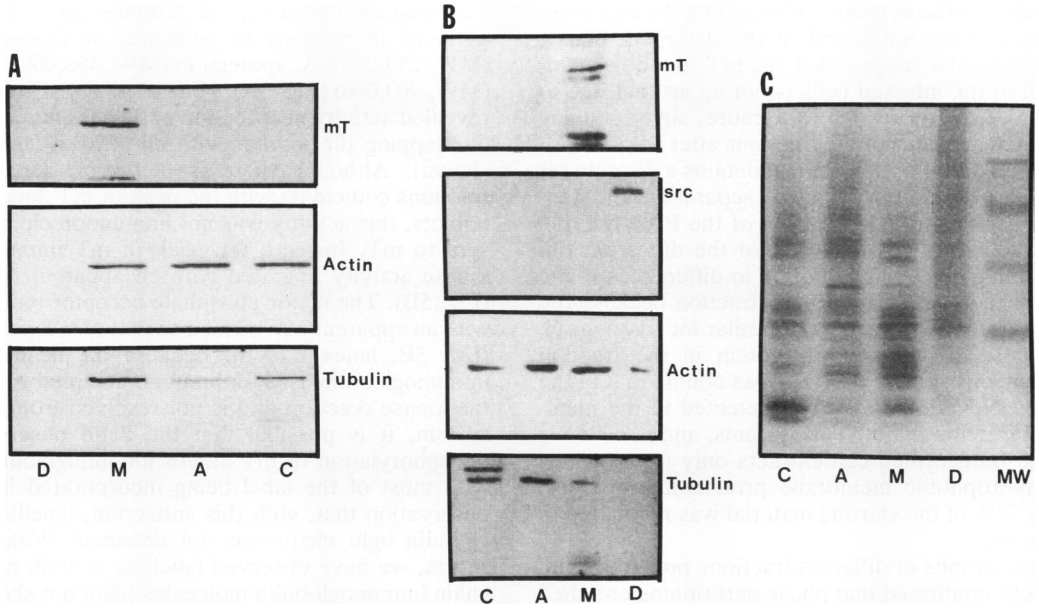

FIG. 3. Phase partitioning of molecules from infected 293 cells and transformed Rat-2 cells. (A) P100 fraction (125 μg) prepared from infected 293 cells was solubilized in a solution containing TX-114 and glycerol. After removal of the cytoskeleton (lane C) by centrifugation at 14,000 × *g* for 10 min, detergent and aqueous phases were separated by elevating the temperature to 30°C. Membrane skeleton (lane M) was removed from the aqueous phase by centrifugation at 150,000 × *g* for 30 min. The supernatant (lane A) contains soluble hydrophilic proteins from the aqueous phase. The detergent phase (lane D) contains soluble hydrophobic proteins. The recovered proteins were solubilized in 50 μl of SDS-PAGE loading buffer, and 10 μl of each fraction was analyzed in each lane on the gel. After transfer of SDS-PAGE-separated proteins to nitrocellulose, mT was detected with a polyclonal antiserum to mT or monoclonal antibodies to actin and tubulin and alkaline phosphatase-conjugated secondary antibodies. The region from approximately 75 to 35 kDa is shown for each blot. (B) The distribution of proteins in transformed Rat-2 cells was determined for the same fractions (C, A, M, and D) as for panel A, except that two samples of the P100 fraction (120 μg each) were processed. One set of fractions was solubilized in 20 μl of SDS-PAGE loading buffer and was analyzed for mT. The other set of fractions was solubilized in 50 μl of loading buffer, and 10 μl of each fraction was analyzed as for panel A. In addition, pp60$^{c\text{-}src}$ was detected by probing the blot with a specific polyclonal antiserum. The lower-MW band in lane M of the blot probed with antiserum to mT is presumed to result from degradation of mT, because prolonged incubation of the fractions resulted in a decrease in the intensity of the higher-MW band and an increase in that of the lower-MW band. The origin of the upper cross-reactive band in lane C of the blot developed with a monoclonal antibody to tubulin (upper band) is unknown and was not observed with infected 293 cells. (C) Total proteins in fractions prepared from infected 293 cells. Polypeptides were visualized by silver staining of the SDS-PAGE gel. Approximately 2 μg of protein was analyzed in each lane. Fractions C, A, M, and D are the same as in panel A. Marker proteins migrate at MWs of 110,000, 84,000, 47,000, and 33,000. The gel system has been optimized for the region between MWs of 70,000 and 10,000. The estimated MW for mT by this gel system is 58,000.

and vimentin were detected in roughly equal amounts in both the supernatant and pellet fractions (Fig. 2, lanes 3 to 5 and 8 to 10, respectively).

Phase partitioning of mT complexes. To separate cytoskeleton markers from integral membrane proteins, we used detergent phase partitioning. Many integral membrane proteins are found to partition with the detergent after solubilization in TX-114 and separation of the detergent and aqueous phases by elevating the temperature from 4°C to 30°C (8). Detergent solubilization and phase partitioning of mT were examined both biochemically and morphologically. P100 fractions of infected 293 cells and mT-transformed Rat-2 cells were solubilized in buffer containing TX-114 and glycerol. The cytoskeleton was removed by centrifugation, and the supernatant was partitioned into aqueous and detergent phases. Membrane skeleton was isolated from the aqueous phase by centrifugation or by velocity sedimentation in sucrose gradients. With this approach, P100 fractions were divided into four fractions (Fig. 3) enriched for cytoskeleton (C), membrane skeleton (M), and the hydrophilic (A) and hydrophobic (D) soluble proteins. After phase separation, 40% of the P100 membrane fraction protein recovered was found in the fraction containing hydrophilic soluble proteins. We presume that most of these proteins are derived from vesicle contents. The remaining 60% of the proteins in the P100 fraction were equally distributed (within 5% of the total) between the other fractions (C, M, and D).

When infected 293 cells were analyzed by immunoblotting, most of the mT was detected in membrane skeleton fractions (Fig. 3A). Because 75% of the proteins in the postnuclear supernatant remain in the S100 fraction, recovery of essentially all of the mT in the fraction enriched for membrane skeleton represents at least a 20-fold enrichment for mT. As expected, actin and tubulin were detected in both membrane skeleton and cytoskeleton fractions (Fig. 3A). Actin was also observed in the fraction containing primarily aqueous soluble proteins (Fig. 3A). When Rat-2 cells transformed with mT were analyzed, the results were, in general, similar to those with 293 cells (Fig. 3B). In these cells, mT was detected in the fraction enriched for membrane skeleton, while the membrane protein pp60$^{c\text{-}src}$ was observed primarily in the detergent phase (Fig. 3B). We cannot determine unambiguously which fraction contains mT complexed to pp60$^{c\text{-}src}$, because only a small fraction of the molecules are in complexes. For these blots, it was necessary to load at least five times more protein on the gel to

detect mT relative to the cytoskeletal markers. As expected, actin and tubulin were not found in the detergent phase. Together, these results suggest that the mT found in membrane skeleton in the infected cells is not an artifact due to overexpression of the protein. Furthermore, silver staining of the total proteins in each of the fractions after SDS-PAGE (Fig. 3C) confirmed that each fraction contains a discrete set of polypeptides. Therefore, the phase separation and centrifugation steps resulted in separation of the P100 fraction into distinct fractions. It is unlikely that the differences in protein partitioning observed were due to differences in the amount of nonspecific protein in each fraction because the amounts of total protein in each were similar for fractions C, M, and D, while the amount of protein in the fraction enriched for aqueous soluble proteins was double that of the other fractions. Nevertheless, mT is detected in the membrane skeleton fraction in both cell systems, and $pp60^{c\text{-}src}$ is detected in the transformed cell extracts only in the detergent phase (hydrophobic membrane proteins). Moreover, approximately 75% of the starting material was recovered in the four fractions.

Electron micrographs of different fractions prepared from infected 293 cells confirmed that phase partitioning enriched for material resembling membrane skeleton (Fig. 4). As expected, the starting P100 fraction contained a variety of different membrane-bound vesicles (Fig. 4A). However, after solubilization with TX-114, there was no longer evidence of membrane structures (Fig. 4B). Although there were structures reminiscent of vesicles in this fraction (Fig. 4B, V arrowheads), at higher magnification (Fig. 4B, inset) they appeared to be surrounded with a fibrous rather than a bilayer structure. Cytoskeletal elements isolated from the solubilized P100 are characterized by bundles of filamentous material (Fig. 4C, F arrowhead). The diameter of the individual filaments in these bundles is 10 to 15 nM. In addition, this fraction contains fibrous material (Fig. 4C, f arrowhead) and dense aggregates (Fig. 4C, D arrowhead). The fraction containing membrane skeleton (isolated by phase partitioning and centrifugation) is characterized by a large number of fibrous structures (Fig. 4D) as well as most of the virus used to infect cells (Fig. 4D, Ad arrowheads) and some poorly resolved aggregates. It is not surprising that material morphologically similar to the fibrous structures in the membrane skeleton is also found in the cytoskeleton fraction (Fig. 4C, f arrowhead) because the two systems are connected.

We used three criteria to distinguish mT complexed with polypeptides of the membrane skeleton from nonspecific aggregates. (i) Complexes contained only a small percentage of the total protein in the TX-114 aqueous phase. (ii) mT migrated in sucrose gradients as a complex of proteins smaller than nonspecific aggregates. (iii) The migration of mT complexes was altered by reagents known to alter the cytoskeleton. It was determined empirically that velocity sedimentation at 115,000 × *g* in gradients containing 10 to 60% sucrose yielded an acceptable separation pattern for this analysis. After centrifugation for as little as 1.5 h, most of the mT is separated from the bulk of the proteins in the TX-114 aqueous phase (data not shown). Alterations in pH or concentration of the TX-114 aqueous phase (with a Centricon concentrator) resulted in nonspecific aggregation, whereupon most of the mT was found at the bottom of the gradient after 1.5 h (data not shown).

Longer separation times (6 h) revealed that mT complexes are somewhat heterogeneous, with apparent MWs ranging from approximately 500,000 to 1,000,000 (Fig. 5, panel A). The migration positions of proteins used as MW markers (assayed in parallel) are indicated as follows: C, catalase (MW, 250,000); A, apoferritin (MW, 450,000); and F, ferritin (MW, 900,000) (Fig. 5A). Kinase assays of gradient fractions revealed activity near the top of the gradient and in fractions overlapping the marker with an MW of 900,000 (data not shown). Although there is detectable kinase activity in fractions coinciding with the peak of mT detected on immunoblots, this activity was not immunoprecipitable with antisera to mT. Instead, the peak of mT immunoprecipitable kinase activity migrated with an apparent MW of 250,000 (Fig. 5B). The major phosphate acceptor resulted in a band with an apparent MW similar to that of mT (55,000 to 59,000) (Fig. 5B, lanes 1 to 6). Because the heavy chain of the immunoglobulin used for immunoprecipitation is in excess in the kinase reaction and is not resolved from mT in our gel system, it is possible that the band observed is due to phosphorylation of mT and/or immunoglobulin. Consistent with most of the label being incorporated into mT is our observation that, with this antiserum, labelling of immunoglobulin light chain was not detected. With another antiserum, we have observed labelling of both heavy and light chain immunoglobulin molecules (data not shown). It is also possible that the kinase activity in any of the gradient fractions was modulated by other proteins that coprecipitated with mT. However, mT immunoprecipitable kinase activity was not detected when uninfected 293 cells were analyzed in parallel (Fig. 5C), suggesting that the kinase activity was specific to mT. Staining of the gels with Coomassie blue (not shown) confirmed that equal amounts of antibody were recovered from each gradient fraction in both panels (Fig. 5B and C). Experiments to address the nature of the specific kinase activity in the various gradient fractions in detail are in progress. Nevertheless, our observation that the peak of mT immunoprecipitable kinase activity migrates in sucrose gradients as a 250-kDa complex is in good agreement with earlier reports (23).

Both DNase I and nocodazole have been widely used to depolymerize cytoskeleton (26). Therefore, the TX-114 aqueous phase prepared from infected 293 cells was incubated with 0.5 mg of DNase I per ml and 25 μg of nocodazole per ml prior to sedimentation on sucrose gradients. The migration of mT in the sucrose gradient was dramatically reduced by this treatment, because the molecule is now detected near the top of the gradient (compare Fig. 6A, lanes 1 to 4, with Fig. 7A, upper panel). However, mT is still detectable further down in the gradient (Fig. 6A, lanes 5 to 10). Therefore, we examined the effectiveness of DNase I and nocodazole for depolymerizing membrane skeleton complexes. The reagents were added to the post-cytoskeleton aqueous phase prepared from infected 293 cells by extraction with TX-114. After incubation for 45 min at 37°C, the remaining membrane skeleton was pelleted as described above. As expected, actin is not released from the membrane skeleton by nocodazole (Fig. 6B, upper panel). However, some actin is released by DNase I, and this effect is slightly augmented by nocodazole (Fig. 6B, upper panel). In contrast, only a small fraction of the tubulin is released by the combination of the two reagents (Fig. 6B, lower panel). Therefore, it appears that the altered migration observed for mT complexes (Fig. 6A, lanes 1 to 4) after exposure to DNase I and nocodazole is primarily due to depolymerization of actin filaments.

In contrast to the depolymerizing activities of DNase I and nocodazole, phalloidin binds to actin filaments and thereby increases the apparent MW of complexes containing actin

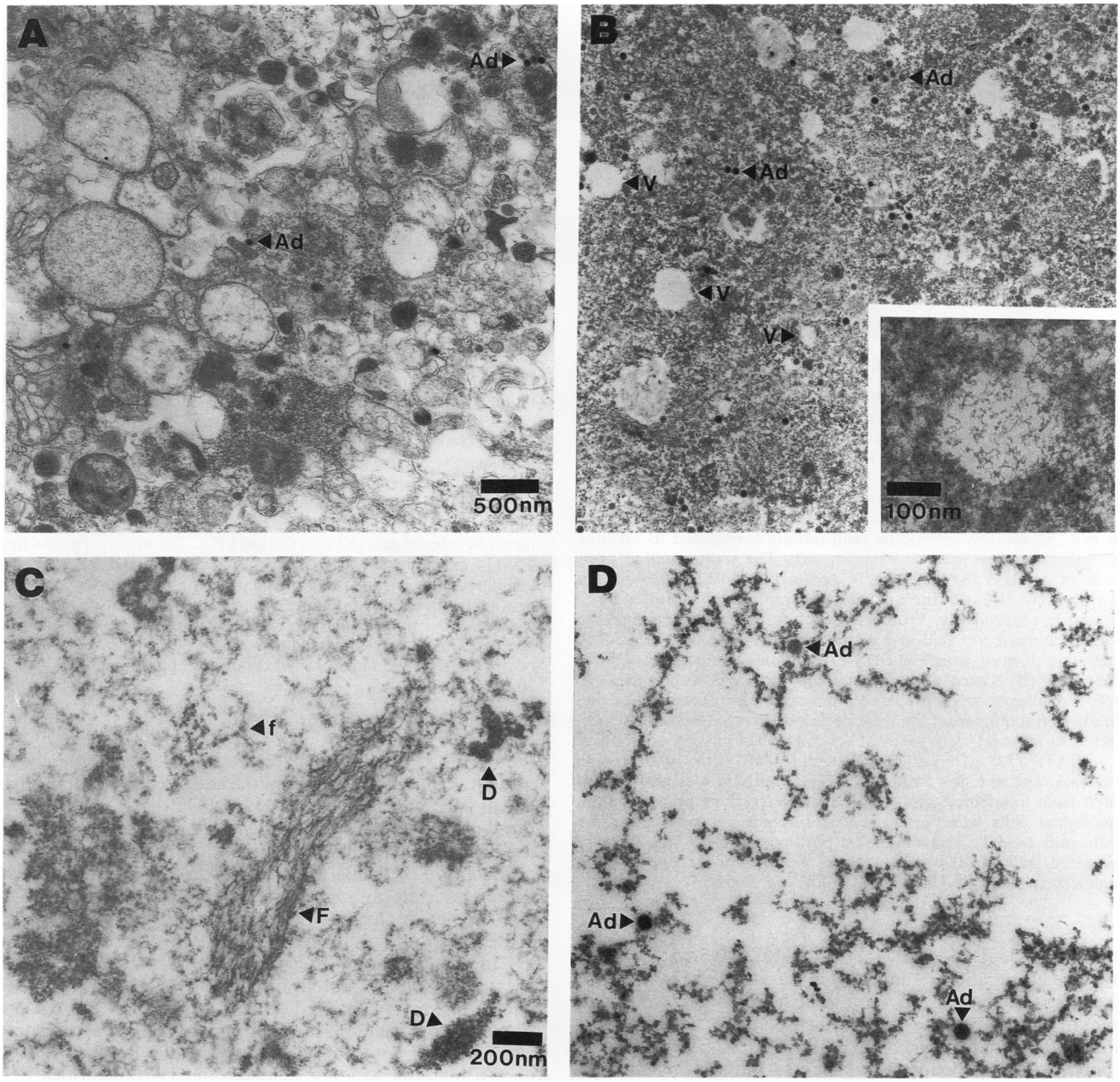

FIG. 4. Electron micrographs of fractions from infected 293 cells. (A) P100 fraction prepared 18 h postinfection. (B) Material pelleted from P100 fraction solubilized in 1.0% TX-114 after 30 min at 100,000 × *g*. Bilayer membranes are not observed surrounding vesicular structures (V arrowheads [also see inset]). (C) The cytoskeleton fraction isolated from a P100 fraction after solubilization in TX-114 and glycerol contains filamentous (F arrowhead) and fibrous (f arrowhead) structures. Dense structures (D arrowheads) may be transverse sections of filamentous structures or aggregates. (D) The membrane skeleton isolated by phase partitioning of post-cytoskeleton detergent-solubilized P100 fraction contains primarily fibrous structures and the virus used to infect cells (Ad arrowheads). Scale bars in panels A and C also apply to panels B and D, respectively.

(14). Therefore, 0.05 mg of phalloidin per ml was added to the TX-114 aqueous phase before sedimentation in sucrose as described above. As expected, binding of phalloidin to actin shifted the migration of the molecule in the gradient (Fig. 7A). Similarly, the bulk of mT in the TX-114 aqueous phase originally detected in fractions 5 to 10 was primarily found in fractions 9 to 12 after phalloidin was added (Fig. 7A). To unambiguously identify both actin and mT on immunoblots, we used a double-staining procedure in which the secondary antibodies used to detect mT and actin (rabbit and mouse, respectively) were conjugated with alkaline phosphatase and horseradish peroxidase, respectively (48). This procedure results in purple bands for alkaline phosphatase and reddish-brown bands for horseradish peroxidase.

The protein content of each fraction of the gradient was analyzed by silver staining after SDS-PAGE. The addition of phalloidin changed the migration position for many but not

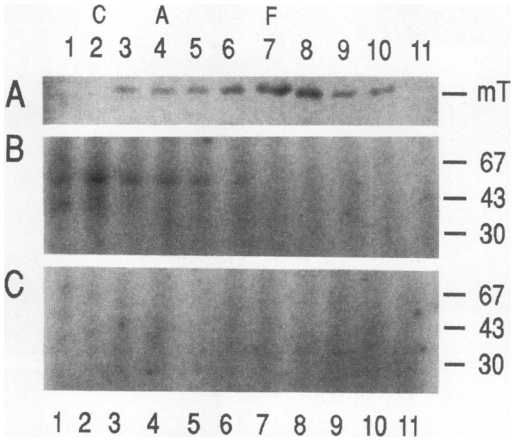

FIG. 5. Sedimentation of mT complexes and mT-associated kinase activity in sucrose gradients. Complexes containing mT were separated from post-cytoskeleton detergent-solubilized P100 fractions by phase partitioning. The aqueous phase, containing mT complexes, was layered onto 10 to 60% sucrose gradients. After sedimentation at 115,000 × *g* for 6 h, the gradients were divided into 11 equal fractions. (A) Immunoblot probed with polyclonal antisera to mT. Secondary antibodies (anti-rabbit) conjugated to alkaline phosphatase were used to visualize mT. The sedimentation positions of catalase (MW, 250,000), apoferritin (MW, 450,000), and ferritin (MW, 900,000) run on a parallel gradient are indicated as C, A, and F, respectively. Proteins in each fraction were precipitated with trichloroacetic acid and were separated by SDS-PAGE. The migration position of mT in SDS-PAGE is indicated at the right of the panel. (B) Kinase activity immunoprecipitable with antisera to mT. Complexes were prepared from Ad5/mT-infected 293 cells. Gradient fractions were immunoprecipitated with a polyclonal antiserum to mT and were assayed for kinase activity by addition of [γ-^{32}P]ATP (5.0 μCi per fraction) and $MnCl_2$ (to 10 mM) and incubation at 30°C for 5 min. (C) Kinase activity was not precipitated from uninfected 293 cells. Gradient fractions prepared from uninfected cells were processed as for panel B with the same antiserum to mT. The migration positions of MW markers are indicated (MW, 67,000 to 30,000) to the right of the figure. Lane numbers are indicated above and below the panels.

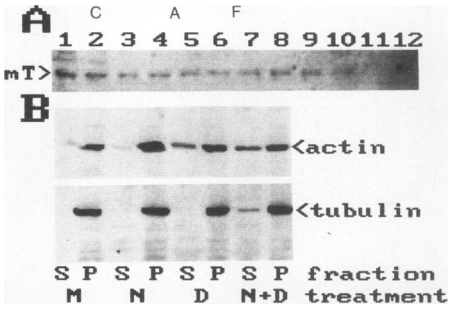

FIG. 6. Sedimentation of mT in sucrose gradients is reduced after incubation with DNase I and nocodazole. (A) The aqueous phase from TX-114 extraction of P100 fraction of infected 293 cells was incubated with DNase I and nocodazole for 45 min prior to sedimentation and immunoblotting as described in the legend to Fig. 5. After sedimentation at 115,000 × *g* for 6 h, the gradients were divided into 12 equal fractions. The sedimentation positions of catalase (MW, 250,000), apoferritin (MW, 450,000), and ferritin (MW, 900,000) run on a parallel gradient are indicated as C, A, and F, respectively. The migration position of mT is indicated to the left of the figure. The region of the blot shown encompasses MWs from approximately 90,000 to 45,000. (B) Release of actin (top panel) and tubulin (bottom panel) from membrane skeleton (M; mock treatment) by nocodazole (N) and DNase I (D). The aqueous phase from TX-114 extraction of a P100 fraction from infected 293 cells was incubated with DNase I and nocodazole for 45 min prior to centrifugation (as described in the legend to Fig. 3) to separate membrane skeleton (P) from soluble proteins (S). The migration positions of actin and tubulin are indicated to the right of the figure. The regions of the blots shown encompass MWs from approximately 90,000 to 30,000.

all polypeptides (Fig. 7B, lanes 4 to 12). Two polypeptides for which migration is unchanged are identified by a dot to the left of the bands. To identify specific polypeptides with migration shifts consistent with association with mT, the species detected in lanes 7 and 10 were compared for each panel. When phalloidin was added to the sample, the patterns of polypeptides in lanes 7 and 10 were very similar (Fig. 7B, lower panel). However, examination of the untreated sample revealed several peptides in lane 7 that are not found in lane 10. Three of these are indicated with arrowheads to the right of the figure. The pattern of proteins in lane 7 of the untreated sample is similar to that reported above for membrane skeleton pellets.

DISCUSSION

The subcellular localization of mT has been investigated by cell fractionation and electron microscopy. Using a procedure designed to isolate membrane skeleton from a P100 fraction, we have identified a complex containing mT that can be isolated from infected 293 cells. This complex migrates in sucrose gradients as a relatively homogeneous species (on the basis of the protein profile in silver-stained gels) with an estimated MW of 500,000 to 1,000,000. Although mT is usually considered to be an integral membrane protein, it was recovered from the aqueous phase after phase partitioning with TX-114. It is possible that a subset of the proteins associated with mT in the complexes described here are relatively hydrophilic and, therefore, control partitioning of the entire complex. For this reason, our partitioning data cannot be used to suggest that any individual component of the complex (including mT) is or is not an integral membrane protein. In addition to this complex, a small fraction of the mT in a P100 fraction prepared from infected 293 cells was present as soluble protein in both the detergent phase and aqueous phase from TX-114 separations (Fig. 3). We presume that this material results from the high level of expression obtained with the adenovirus system because uncomplexed material was not detected in mT-transformed cells (Fig. 3). To obtain a relatively monodisperse species and prevent aggregation during phase partitioning, it was necessary to include a panel of protease inhibitors as well as to optimize the ionic strength (150 to 300 mM NaCl) and glycerol concentration (5 to 10%) of the solubilization buffer. Furthermore, deviations in pH or concentration of the aqueous phase resulted in aggregation of the sample.

In contrast to the complex characterized here, mT complexes isolated from different cell types by a variety of procedures have been described as heterodisperse (MW range, 50,000 to the bottom of the gradient), with the peak kinase activity migrating near an MW of 200,000 (23). In agreement with our results (Fig. 5), sedimentation of cell extracts from [^{35}S]Met-labelled cells indicated that much of the immunoprecipitable mT migrated with an estimated MW considerably higher than the peak of kinase activity in these preparations (23). However, the composition of the high-MW material was not explored.

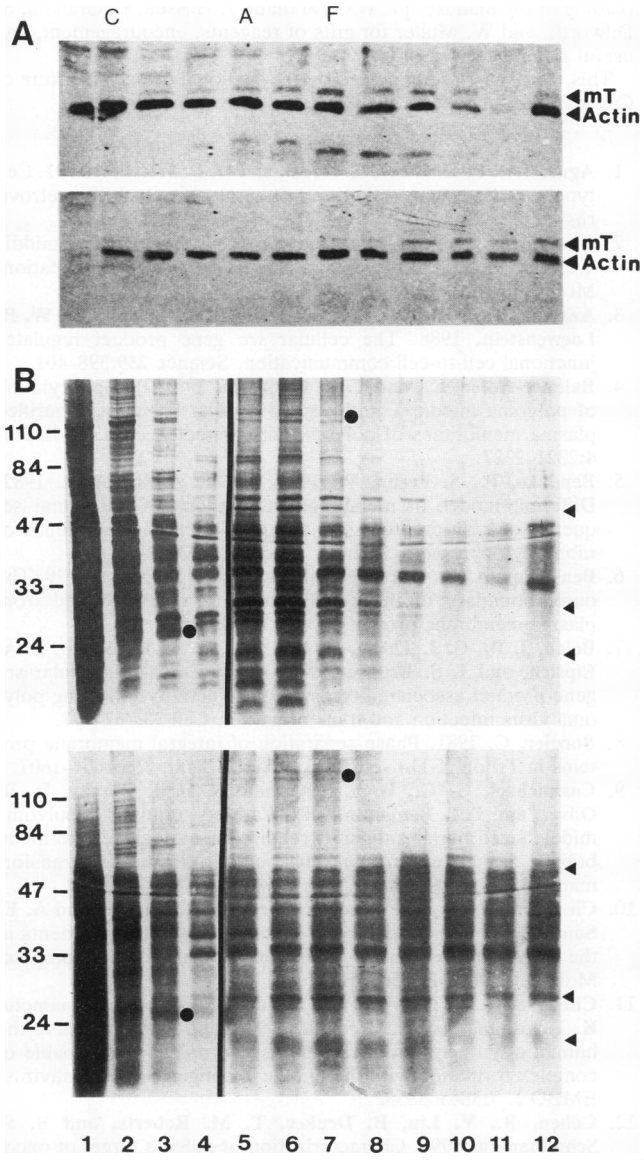

FIG. 7. Sedimentation of mT complexes in sucrose gradients. (A) The aqueous phase from TX-114 extraction of P100 from infected 293 cells was analyzed by sedimentation in sucrose gradients and immunoblotting as described above (upper blot) or after incubation with phalloidin (lower blot). Immunoblots for mT and actin were detected with alkaline phosphatase and horseradish peroxidase-conjugated secondary antibodies, respectively. The sedimentation positions of catalase (MW, 250,000), apoferritin (MW, 450,000), and ferritin (MW, 900,000) run on a parallel gradient are indicated as C, A, and F, respectively. (B) Total proteins from the gradients in panel A visualized by silver staining. The first four lanes in each gel were printed with a shorter exposure to improve image clarity. Upper and lower gels are without and with phalloidin, respectively. Dots are positioned to the right of bands from polypeptides not shifted by phalloidin. Arrowheads indicate the migration positions of polypeptides with altered migration after the addition of phalloidin. The migration positions of mT, actin, and MW markers (MW, 110,000 to 24,000) are indicated to the sides of the figure.

It has been reported that mT associates with a number of cellular proteins, including *src* family protein tyrosine kinases (MW ≈ 60,000), the 81- to 85-kDa subunit of PI-3-kinase, the A and C subunits of protein phosphatase 2A (MWs, 61,000 and 37,000, respectively) and two uncharacterized polypeptides with MWs of 88,000 and 110,000. If one of the members of the tyrosine kinase family and all of the other components known to interact with mT were present in a single complex, the predicted MW would be almost 500,000. However, on the basis of recent data on the stoichiometry of cellular tyrosine kinases, p81/85, and mT in complexes, it is also possible that mT forms a number of different complexes (10). These complexes are envisioned as having different biological effects and potentially different MWs. However, our results suggest that these complexes either contain a small amount of the total mT expressed in the cell or have similar MWs (500,000 to 1,000,000). Consistent with the former suggestion is our observation that the peak of mT immunoprecipitable kinase activity does not comigrate with the majority of mT in sucrose density gradients (Fig. 5).

Recent approaches to the isolation of mT complexes have employed antibodies directed against one or more of the proteins present in putative complexes (10, 22, 36). However, it is possible that this approach may result in partial fragmentation of physiologically relevant complexes, especially because cells are typically lysed in 1% Nonidet P-40. Consistent with this view and with the potential interaction of mT with either cytoskeleton or membrane skeleton is the observation of substoichiometric amounts of actin in immunopurified mT complexes (22, 36). Although a limited number of polypeptides were observed to cofractionate with mT after the detergent phase separation used here, identification of the individual polypeptides which make up the species with MWs of 500,000 to 1,000,000 awaits further purification of the complex. Nevertheless, in contrast to the MWs of immunopurified complexes, the MW of the mT complex identified here is large enough to accommodate many of the polypeptides known to interact with mT as well as regulatory proteins and a putative adaptor molecule for membrane skeleton association.

Interaction of mT with membrane skeleton (in addition to or instead of with cellular membranes directly) can potentially explain the discrepancies obtained when the location of mT is assessed morphologically and biochemically. Immunofluorescence and immunoelectron microscopy indicate that a large fraction of mT is coincident with intracellular membranes such as endoplasmic reticulum and Golgi apparatus (18, 47, 55). In contrast, data from other biochemical approaches have been interpreted to suggest that mT resides primarily in the plasma membrane (4, 28, 41, 44). Both results can be accommodated by localization of mT on membrane skeleton, provided that membrane skeleton released from various subcellular organelles cofractionates with plasma membrane. Although this possibility requires further investigation, there is some indication that plasma membrane fractions might contain membrane skeleton. For example, mT was presumed to be found in the plasma membrane after enrichment for membrane fractions by using elevated pH (4). However, as shown in Fig. 2, elevated pH can cause mT and the membrane skeleton to aggregate on membrane fractions. Other reports suggest that after hypotonic lysis, mT is associated with membrane vesicles that sediment rapidly in sucrose gradients (presumed plasma and nuclear membrane [44]). Because these conditions only partially separate membrane skeleton from either cytoskel-

eton or membranes, it is likely that membrane skeleton is present in heavy membrane fractions.

Although the cell fraction shown here to contain most of the cellular mT resembles membrane skeleton both biochemically and morphologically (6, 20), little is known about this filamentous system. Membrane skeleton has been studied primarily with erythrocytes, which lack membranes other than the plasma membrane. However, micrographs of membrane skeleton from platelets (20) and other cell types (6, 27) reveal fibrous structures that are remarkably similar to the structures observed in this study (Fig. 4). Our observation that tubulin, actin, and vimentin can all be detected in the mT-enriched fractions is also consistent with attachment of the mT complex to the membrane skeleton. Most striking is our observation that the migration of mT complexes in sucrose gradients is shifted in response to reagents known to alter cytoskeleton (Fig. 6 and 7). Although we do not interpret these data as suggesting that mT binds to actin, they do indicate that there is actin associated with the mT complexes in the TX-114 aqueous phase. Finally, our results are also consistent with an earlier report that about half of the total mT in polyomavirus-transformed 3T3 cells is associated with the detergent-insoluble framework (membrane skeleton and cytoskeleton were not separated) of the cell (41). However, we find that in transformed Rat-2 cells, all of the mT detectable is present in fractions enriched for membrane skeleton. It seems likely that apparent differences in distribution are due to the low ionic strength (and lack of glycerol) in the solubilization buffer used previously (41), which would only partially release membrane skeleton from the cytoskeleton.

The interaction between mT and membrane skeleton identified here with both transformed Rat-2 and infected 293 cells has implications for the role of mT in transformation. Of the molecules known to be associated with mT in transformed cells, only the *src*-related kinases are normally membrane proteins. Therefore, it is possible that binding to mT directs molecules such as phosphatase 2A and PI-3 kinase to potential targets in the cytoskeletal network.

With the cellular fractionation protocol devised here, $pp60^{c\text{-}src}$ is found primarily in the fraction containing detergent-soluble membrane proteins. However, in some experiments, we found that in transformed Rat-2 cells, a small amount of the cellular $pp60^{c\text{-}src}$ is also found in fractions enriched for membrane skeleton (data not shown). This result is consistent with earlier reports that only a small fraction of the $pp60^{c\text{-}src}$ present in cells is bound to mT. It has been suggested that the novel kinase substrates of v-*src* in transformed cells include cytoskeletal markers such as vinculin (24, 43). Finally, recent experiments with v-*src* redirected to different subcellular locations have demonstrated that localization to adhesion plaques is sufficient for transformation of chicken embryo fibroblasts (30a). In contrast, v-*src* redirected to other subcellular locations was either mitogenic or benign (30a). Both mT and v-*src* have been proposed to interfere with cell-to-cell communication at adherens junctions (2, 3). Adherens junctions are one of the areas in the cell where the cytoskeleton and membrane skeleton are joined (46). Therefore, investigation of the potential role of membrane skeleton-bound mT in alterations in morphology, cell-to-cell communication, and other related processes may provide insight into the mechanism of mT-mediated cellular transformation.

ACKNOWLEDGMENTS

We thank B. Leber, Fabiola Janiak, and Alison Cowie for critical reading of the manuscript. We also thank J. Hassell, F. Graham, S. Dilworth, and W. Muller for gifts of reagents, encouragement, and useful scientific discussions.

This research was supported by the National Cancer Institute of Canada with funds from the Canadian Cancer Society.

REFERENCES

1. **Aguzzi, A., P. Kleihues, K. Heckl, and O. D. Wiestler.** 1991. Cell type-specific tumor induction in neural transplants by retrovirus-mediated oncogene transfer. Oncogene **6**:113–118.
2. **Azarnia, R., and W. R. Loewenstein.** 1987. Polyomavirus middle T antigen downregulates junctional cell-to-cell communication. Mol. Cell. Biol. **7**:946–950.
3. **Azarnia, R., S. Reddy, T. E. Kmiecik, D. Shalloway, and W. R. Loewenstein.** 1988. The cellular *src* gene product regulates junctional cell-to-cell communication. Science **239**:398–401.
4. **Ballmer-Hofer, K., and T. L. Benjamin.** 1985. Phosphorylation of polyoma middle T antigen and cellular proteins in purified plasma membranes of polyoma virus-infected cells. EMBO J. **4**:2321–2327.
5. **Bendzko, P., S. Prehn, W. Pfeil, and T. A. Rapoport.** 1982. Different modes of membrane interactions of the signal sequence of carp preproinsulin and of the insertion sequence of rabbit cytochrome b_5. Eur. J. Biochem. **123**:121–126.
6. **Ben-Ze'ev, A., A. Duerr, F. Solomon, and S. Penman.** 1979. The outer boundary of the cytoskeleton: a lamina derived from plasma membrane proteins. Cell **17**:859–865.
7. **Bolen, J. B., C. J. Thiele, M. A. Israel, L. A. Yonemoto, L. A. Lipsich, and J. S. Brugge.** 1984. Enhancement of cellular src gene product associated tyrosyl kinase activity following polyoma virus infection and transformation. Cell **38**:767–777.
8. **Bordier, C.** 1981. Phase separation of integral membrane proteins in Triton X-114 solution. J. Biol. Chem. **256**:1604–1607.
9. **Carmichael, G. G., B. S. Schaffhausen, D. I. Dorsky, D. B. Oliver, and T. L. Benjamin.** 1982. Carboxy terminus of polyoma middle sized tumor antigen is required for attachment to membranes, associated protein kinase activities, and cell transformation. Proc. Natl. Acad. Sci. USA **79**:3579–3583.
10. **Cheng, S. H., P. C. Espino, J. Marshall, R. Harvey, and A. E. Smith.** 1990. Stoichiometry of cellular and viral components in the polyomavirus middle-T antigen–tyrosine kinase complex. Mol. Cell. Biol. **10**:5569–5574.
11. **Cheng, S. H., R. Harvey, P. C. Espino, K. Semba, T. Yamamoto, K. Toyoshima, and A. E. Smith.** 1990. Peptide antibodies to the human c-fyn gene product demonstrate $pp59^{c\text{-}fyn}$ is capable of complex formation with the middle T antigen of polyomavirus. EMBO J. **7**:3845–3855.
12. **Cohen, B., Y. Liu, B. Druker, T. M. Roberts, and B. S. Schaffhausen.** 1990. Characterization of pp85, a target of oncogenes and growth factor receptors. Mol. Cell. Biol. **10**:2909–2915.
13. **Cook, D. N., N. Pavloff, and J. A. Hassell.** 1990. Simultaneous overexpression of avian $pp60^{c\text{-}src}$ and polyomavirus middle T antigen in mammalian cells. J. Virol. **64**:2392–2395.
14. **Cooper, J. A.** 1987. Effects of cytochalasin and phalloidin on actin. J. Cell Biol. **105**:1473–1478.
15. **Courtneidge, S. A., and A. E. Smith.** 1983. Polyoma virus transforming protein associates with the product of the c-src cellular gene. Nature (London) **303**:435–439.
16. **Dailey, H. A., and P. Strittmatter.** 1978. Structural and functional properties of the membrane binding segment of cytochrome b_5. J. Biol. Chem. **253**:8203–8209.
17. **Dilworth, S. M., and B. E. Griffin.** 1982. Monoclonal antibodies against polyoma virus tumor antigen. Proc. Natl. Acad. Sci. USA **79**:1059–1063.
18. **Dilworth, S. M., H.-A. Hansson, C. Darnfors, G. Bjursell, C. H. Streuli, and B. E. Griffin.** 1986. Subcellular localization of the middle and large T-antigens of polyoma virus. EMBO J. **5**:491–499.
19. **Druker, B., L. E. Ling, B. Cohen, T. M. Roberts, and B. S. Schaffhausen.** 1990. A completely transformation-defective

point mutant of polyomavirus middle T antigen which retains full associated phosphatidylinositol kinase activity. J. Virol. **64**:4454–4461.

20. **Fox, J. E. B., J. K. Boyles, M. C. Berndt, P. K. Steffen, and L. K. Anderson.** 1988. Identification of a membrane skeleton in platelets. J. Cell Biol. **106**:1525–1538.
21. **Fujiki, Y., A. D. Hubbard, S. Fowler, and P. B. Lazarow.** 1982. Isolation of intracellular membranes by means of sodium carbonate treatment: application to endoplasmic reticulum. J. Cell Biol. **93**:97–102.
22. **Grussenmeyer, T., A. Carbone-Wiley, K. H. Scheidtmann, and G. Walter.** 1987. Interactions between polyomavirus medium T antigen and three cellular proteins of 88, 61, and 37 kilodaltons. J. Virol. **61**:3902–3909.
23. **Grussenmeyer, T., K. H. Scheidtmann, M. A. Hutchinson, W. Eckhart, and G. Walter.** 1985. Complexes of polyoma virus medium T antigen and cellular proteins. Proc. Natl. Acad. Sci. USA **82**:7952–7954.
24. **Hamaguchi, M., and H. Hanafusa.** 1989. Localization of major potential substrates of $p60^{v\text{-}src}$ kinase in the plasma membrane matrix fraction. Oncogene Res. **4**:29–37.
25. **Horak, I. D., T. Kawakami, F. Gregory, K. C. Robbins, and J. B. Bolen.** 1989. Association of $p60^{fyn}$ with middle tumor antigen in murine polyomavirus-transformed rat cells. J. Virol. **63**:2343–2347.
26. **Horvath, A. R., L. Muszbek, and S. Kellie.** 1992. Translocation of pp60c-src to the cytoskeleton during platelet aggregation. EMBO J. **11**:855–861.
27. **Ishikawa, H., and N. Fujimaki.** 1986. Electron microscopic observations on the plasmalemmal undercoat, p. 1913–1916. *In* Proceedings of the XIth International Congress on Electron Microscopy. Japanese Society of Electron Microscopy, Tokyo.
28. **Ito, Y., J. R. Brocklehurst, and R. Dulbecco.** 1977. Virus-specific proteins in the plasma membrane of cells lytically infected or transformed by polyoma virus. Proc. Natl. Acad. Sci. USA **74**:4666–4670.

28a. **Janiak, F., et al.** Submitted for publication.

29. **Kornbluth, S., S. H. Cheng, W. Markland, Y. Fukui, and H. Hanafusa.** 1990. Association of $p62^{c\text{-}yes}$ with polyomavirus middle T-antigen mutants correlates with transforming ability. J. Virol. **64**:1584–1589.
30. **Kornbluth, S., M. Sudol, and H. Hanafusa.** 1987. Association of the polyomavirus middle T-antigen with c-yes protein. Nature (London) **325**:171–173.

30a. **Liebl, E. C., and S. Martin.** 1992. Intracellular targeting of $pp60^{src}$ expression: localization of v-src to adhesion plaques is sufficient to transform chicken embryo fibroblasts. Oncogene **7**:2417–2428.

31. **Lin, K.-H., and S.-Y. Cheng.** 1991. An efficient method to purify active eukaryotic proteins from the inclusion bodies in *Escherichia coli*. BioTechniques **6**:748–753.
32. **Ling, L. E., B. J. Druker, L. C. Cantley, and T. M. Roberts.** 1992. Transformation-defective mutants of polyomavirus middle T antigen associate with phosphatidylinositol 3-kinase (PI 3-kinase) but are unable to maintain wild-type levels of PI 3-kinase products in intact cells. J. Virol. **66**:1702–1708.
33. **Markland, W., S. H. Cheng, B. A. Oostra, and A. E. Smith.** 1986. In vitro mutagenesis of the putative membrane-binding domain of polyomavirus middle T antigen. J. Virol. **59**:82–89.
34. **Markland, W., and A. E. Smith.** 1987. Mutants of polyomavirus middle T antigen. Biochem. Biophys. Acta **907**:299–321.
35. **Pallas, D. C., V. Cherington, W. Morgan, J. DeAnda, D. Kaplan, B. Schaffhausen, and T. M. Roberts.** 1988. Cellular proteins that associate with the middle and small T antigens of polyomavirus. J. Virol. **62**:3934–3940.
36. **Pallas, D. C., W. Morgan, and T. M. Roberts.** 1989. The cellular proteins which can associate specifically with polyomavirus middle T antigen in human 293 cells include the major human 70-kilodalton heat shock proteins. J. Virol. **63**:4533–4539.
37. **Pallas, D. C., L. K. Shahrik, B. L. Martin, S. Jaspers, T. B. Miller, D. L. Brautigan, and T. M. Roberts.** 1990. Polyoma small and middle T antigens and SV40 small T antigen form stable complexes with protein phosphatase 2A. Cell **60**:167–176.
38. **Piwnica-Worms, H., N. G. Williams, S. H. Cheng, and T. M. Roberts.** 1990. Regulation of $pp60^{c\text{-}src}$ and its interaction with polyomavirus middle T antigen in insect cells. J. Virol. **64**:61–68.
39. **Rassoulzadegan, M., S. A. Courtneidge, R. Loubiere, P. El Blaze, and F. Cuzin.** 1990. A variety of tumours induced by the middle T antigen of polyoma virus in a transgenic mouse family. Oncogene **5**:1507–1510.
40. **Sabatini, D. D., G. Kreibich, T. Morimoto, and M. Adesnick.** 1982. Mechanisms for the incorporation of proteins in membranes and organelles. J. Cell Biol. **92**:1–22.
41. **Schaffhausen, B. S., H. Dorai, G. Arakere, and T. L. Benjamin.** 1982. Polyomavirus middle T antigen: relationship to cell membranes and apparent lack of ATP-binding activity. Mol. Cell. Biol. **2**:1187–1198.
42. **Schagger, H., and G. Von Jagow.** 1987. Tricine-sodium dodecyl sulfate-polyacrylamide gel electrophoresis for the separation of proteins in the range from 1–100 kDa. Anal. Biochem. **166**:368–379.
43. **Sefton, B. M., T. Hunter, E. H. Ball, and S. J. Singer.** 1981. Vinculin: a cytoskeletal target of the transforming protein of Rous sarcoma virus. Cell **24**:165–174.
44. **Segawa, K., and Y. Ito.** 1982. Differential subcellular localization of in vivo-phosphorylated and nonphosphorylated middle sized tumor antigen of polyoma virus and its relationship to middle sized tumor antigen phosphorylating activity in vitro. Proc. Natl. Acad. Sci. USA **79**:6812–6816.
45. **Serunian, L. A., K. R. Auger, T. M. Roberts, and L. C. Cantley.** 1990. Production of novel polyphosphoinositides in vivo is linked to cell transformation by polyomavirus middle T antigen. J. Virol. **64**:4718–4725.
46. **Simon, K. O., C. A. Otey, F. M. Pavalko, and K. Burridge.** 1991. Protein interactions linking actin to the plasma membrane in focal adhesions, p. 57–64. *In* M. S. Mooseker and J. S. Morrow (ed.), Ordering the membrane-cytoskeleton trilayer. Academic Press, Inc., San Diego, Calif.
47. **Templeton, D., A. Voronova, and W. Eckhart.** 1984. Construction and expression of a recombinant DNA gene encoding a polyomavirus middle size tumor antigen with the carboxyl terminus of the vesicular stomatitis virus glycoprotein G. Mol. Cell. Biol. **4**:282–289.
48. **Theisen, N., E. S. Lohoff, K. von Figura, and A. Hasilik.** 1986. Sequential detection of antigens in western blots with differently colored products. Anal. Biochem. **152**:211–214.
49. **Treisman, R., U. Novak, J. Favaloro, and R. Kamen.** 1981. Transformation of rat cells by an altered polyoma virus genome expressing only the middle T protein. Nature (London) **292**:595–600.
50. **Ulug, E. T., A. J. Cartwright, and S. A. Courtneidge.** 1992. Characterization of the interaction of polyomavirus middle T antigen with type 2A protein phosphatase. J. Virol. **66**:1458–1467.
51. **Wang, R., and V. L. Bautch.** 1991. The polyomavirus early region gene in transgenic mice causes vascular and bone tumors. J. Virol. **65**:5174–5183.
52. **Whitman, M., D. R. Kaplan, B. S. Schaffhausen, L. C. Cantley, and T. M. Roberts.** 1985. Association of phosphatidylinositol kinase activity with polyoma middle T competent for transformation. Nature (London) **315**:239–242.
53. **Wigler, M., A. Pellicer, S. Silverstein, and R. Axel.** 1978. Biochemical transfer of single-copy eucaryotic genes using total cellular DNA as donor. Cell **14**:725–731.
54. **Williams, R. L., W. Risau, H.-G. Zerwes, H. Drexler, A. Aguzzi, and E. F. Wagner.** 1989. Endothelioma cells expressing the polyoma middle T oncogene induce hemangiomas by host cell recruitment. Cell **57**:1053–1063.
55. **Zhu, Z., G. M. Veldman, A. Cowie, A. Carr, B. Schaffhausen, and R. Kamen.** 1984. Construction and functional characterization of polyomavirus genomes that separately encode the three early proteins. J. Virol. **51**:170–180.